Catalysis Letters, Vol. 117, Nos. 3–4, September 2007 (© 2007)
DOI: 10.1007/s10562-007-9131-8

Friedel–Crafts acylation of anisole and toluene with acetic anhydride over nano-sized Beta zeolites

Xiangfei Ji,[a,b] Zhangfeng Qin,[a] Mei Dong,[a] Guofu Wang,[a] Tao Dou,[c] and Jianguo Wang[a,*]

[a]*State Key Laboratory of Coal Conversion, Institute of Coal Chemistry, Chinese Academy of Sciences, P.O. Box 165, Taiyuan, Shanxi, 030001, PR China*
[b]*Graduate University of Chinese Academy of Sciences, Beijing, 100041, PR China*
[c]*CNPC Key Laboratory of Catalysis, University of Petroleum, Fuxue Road, Changping, Beijing, 102249, PR China*

Received 18 April 2007; accepted 18 April 2007

Nano-sized Beta zeolites, with a crystal size of 80–100 nm, were synthesized via surface wet method. The nano-sized HBeta zeolites exhibit much higher activity and stability in the Friedel–Crafts acylation of anisole and toluene with acetic anhydride than the conventional zeolites of large particle size. The small crystal size of nano-sized zeolites may bring on more accessible active sites and then enhance the catalytic activity. The exposed pore openings in nano-sized zeolites allow a fast desorption of heavy products from the catalyst and can then reduce the occupancy of active sites by the adsorption of products; this can then alleviate the catalyst deactivation and improve the catalyst stability.

KEY WORDS: nano-size; Beta zeolites; acylation; anisole; toluene; acetic anhydride.

1. Introduction

The Friedel–Crafts acylation of aromatic compounds is one of the most important routes for the synthesis of aromatic ketones intermediates in the fine chemical and pharmaceutical industry [1]. In a conventional homogenous process, aromatics and carboxylic acid derivatives are used as reactants and Lewis acid anhydrous metal halides as catalysts, which may cause serious corrosion and pollution problems [2]. Therefore, considerable efforts have been made to develop heterogeneous processes using solid acid catalysts such as zeolites, clays and heteropolyacids [3–10]; of them, especially, zeolites combine acidic properties with shape selectivity and exhibit accordingly good catalytic activity and selectivity in the acylation of aromatic compounds. However, the solid acid as acylation catalyst often suffers from fast deactivation and then needs frequent regeneration, mainly owing to the stable adsorption of heavy products and the permanent deposition of carbonaceous substances on the catalyst that may block the accesses that reactants need to the active sites in the catalyst [11].

Zeolites with a small particle size have exhibited attractive performances in a series of catalytic reactions such as hydrocracking of crude oil, hydroxylation of phenol, isomerization of xylene, and oligomerization of ethylene [12–15]; the decrease in the crystal size of zeolites can effectively improve their catalytic activity and stability. It is then expected that both activity and stability may be improved by using the zeolites of small crystal size and large external surface as catalysts in the Friedel–Crafts acylation, because the small-sized zeolites can bring on more accessible active sites and the exposed pore openings allow a fast diffusion and desorption of heavy products from the catalysts. However, there are few reports concerning the application of nano-sized zeolites in the Friedel–Crafts acylation.

In this work, the nano-sized Beta zeolites were synthesized and used as catalysts in the Friedel–Crafts acylation of anisole and toluene with acetic anhydride. The influences of particle size on the catalytic performances were investigated through comparing acylation reaction behaviors over HBeta zeolites of different sizes from nanometers to micrometers.

2. Experimental

2.1. Zeolites synthesis

For the synthesis of zeolites, tetraethylammonium hydroxide (TEAOH) (mass fraction $w > 25.0\%$) from Tianjin Guangfu Institute of Fine Chemistry, NaOH ($w > 96.0\%$) and sodium metaaluminate $NaAlO_2$ ($Al_2O_3 > 41.0\%$) from Tianjin Hengxing Chemical Reagent Co., and silica gel ($SiO_2 > 96.3\%$) provided by Qingdao Haiyang Chemical Plant were used.

The nano-sized (denoted as β_S) and medium sized (denoted as β_M) Beta zeolites were synthesized via surface wet method by controlling the content of

*To whom correspondence should be addressed.
E-mail: iccjgw@sxicc.ac.cn

1011-372X/07/0900–0171/0 © 2007 Springer Science+Business Media, LLC

TEAOH [16]. The molar composition of the precursor solution for nano-sized Beta is 1.95 Na_2O:3.8 TEAOH:33 SiO_2:1 Al_2O_3:100 H_2O, while for the medium sized Beta zeolites it is 1.95 Na_2O: 2.8 TEAOH:33 SiO_2:1 Al_2O_3:100 H_2O. After intensive stirring for 0.5 h at room temperature, the precursor solution was introduced into a 100 ml Teflon-lined stainless steel autoclave and crystallized at 170 °C for 26 h. After that, the as-synthesized zeolites were filtered, dried at 120 °C overnight and calcined at 550 °C for 6–12 h.

For comparison, Beta zeolites of large particle size (denoted as β_L) were also prepared by nucleation gel method with the molar composition of the precursor solution being 3.1 Na_2O:33 SiO_2:1 Al_2O_3:6.0 TEAOH:15 $(NH_4)_2O$:650 H_2O [17].

Beta zeolites as-synthesized were ion-exchanged with NH_4NO_3 (1 M, 150 ml for 10 g zeolite sample) at 90 °C to obtain NH_4-form samples, which were calcined in air at 550 °C for 3 h to obtain H-form zeolites HBeta. The powder zeolites were further tableted and crushed to granules of 0.4–1 mm for catalytic tests.

2.2. Catalyst characterization

XRD characterization was performed on a powder X-ray diffractometer (Shimadzu 6100) with a monochromated CuKα radiation source (0.15418 nm, 40 kV and 30 mA). Relative crystallinity was extracted by using the most intense diffraction peak at 2θ of 22.5°, taking the integrated intensities of sample β_M as the standard 100 [18].

BET surface area of the catalysts was measured by nitrogen adsorption at −196 °C with ASAP 2000 (Micromeritics Instrument Co.). The samples were degassed at 200 °C and 6.7 Pa for 2 h prior to the measurement.

NH_3-TPD was conducted on a multiple adsorption apparatus TP 5000-II (Tianjin Xianquan Corporation of Scientific Instruments). The measurement was performed in a quartz microtubular reactor. For each run, about 50 mg sample (40–60 mesh) was first pretreated in an argon flow (30 ml/min) at 550 °C for 2 h and then cooled down to 100 °C. NH_3 was then injected to the reactor to start the NH_3 adsorption. After the sample was saturated with NH_3 adsorption, the excessive NH_3 was swept away with the argon flow at 120 °C for 30 min. Then the NH_3-TPD is performed from 120 to 700 °C with a heating rate of 10 °C; the signal of NH_3 desorption was detected by a thermal conductivity detector at the outlet and the effluent was further introduced to an aqueous HCl solution to absorb the desorbed NH_3 that can be titrated by NaOH solution to measure the density of acid sites.

Transmission electron microscopy (TEM) was performed at a JEM-2000EX microscope operated at 200 kV. For TEM analyses, the samples were prepared by sonicating in ethanol for 5 min, followed by depositing one drop of the resulted suspension on a holey copper grid.

UV–VIS spectra were measured with a UV–VIS spectrometer (CARY 300, with an integrated sphere CA-30I, Varian).

Thermogravimetric analysis combined with mass spectra (TG-MS) was carried out on a thermogravimeter (TGA 92, Setaram Co.) under air (40 ml/min) within the temperature range of 30–800 °C at a heating rate of 10 °C/min, and the effluent was monitored with a mass spectrometer (QEM 200).

2.3. Reaction and analytical procedures

For the catalytic tests and analysis, anisole ($w > 98.0\%$), toluene ($w > 98.0\%$), *p*-methylacetophenone (*p*-MAP, $w > 98.0\%$) and *p*-methoxyacetophenone (*p*-MOAP, $w > 98.0\%$) from Shanghai Chemical Reagent Corporation, and acetic anhydride ($w > 98.6\%$) provided by Tianjin Tian-Da Chemical Corporation were used.

The acylation of toluene with acetic anhydride was carried out in a 20 ml stainless steel autoclave equipped with a stirrer. Before each test, 0.1 g catalyst (calcined HBeta zeolites), 60 mmol toluene and 6 mmol acetic anhydride were charged into the autoclave. The mixture was then stirred intensively at 130 °C and 0.13 MPa for a period of 3 h. After that, the reactor was cooled down and the resultants were subjected to analysis with a FID gas chromatograph (Shimadzu GC-14B) equipped with a 60 m × 0.25 mm OV-101 capillary column.

The acylation of anisole with acetic anhydride was carried out in a fixed-bed reactor with an inner diameter of 6 mm and length of 300 mm. About 0.5 g catalyst was loaded for each test, and a flow of N_2 (23 ml/min) was used as a carrier and diluting gas. The reactant mixture with a molar ratio of anisole to acetic anhydride being 5 was pressurized to the reactor by a metering pump with a liquid flow rate of 5 ml/h. The reaction was conducted at 3.7 MPa and 120 °C. The effluents were decompressed through a backpressure regulator, and liquid products and unreacted reactants were condensed in a trap with an ice water bath, which were then analyzed with the gas chromatograph.

3. Results and discussion

3.1. Beta zeolites of different particle sizes

Beta zeolites with different particle sizes varied from 60 to 4000 nm were synthesized. As shown by the XRD patterns in figure 1, the characteristic diffraction peaks at 2θ of 7.8° and 22.5° suggest that the as-synthesized Beta zeolites have the structure of BEA with high crystallinities and there are no visible peaks from any impurities. This proves that the surface wet method is an effective way to prepare Beta zeolites with high

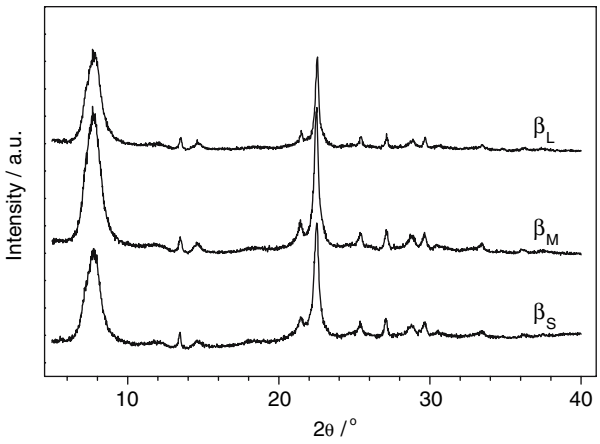

Figure 1. XRD patterns of the as-synthesized Beta zeolites (β_S, nano-sized; β_M, medium sized; β_L, large sized).

crystallinity. It has been proposed that high concentration of templates and high alkalinity of precursor, formed by the surface wet method, can accelerate the dissolution of aluminasilica and the formation of crystal nuclei [19].

Figure 2 shows the TEM micrographs of the as-synthesized zeolites, from which their particle sizes can be estimated. β_S crystals are irregular in the shape and the particle size ranges from 60 to 100 nm. β_M and β_L appear to be round in the shape and their particle sizes are in the range of 210–300 nm and 2.3–4.0 μm, respectively. Moreover, the aggregation of particles is not evident, as suggested by the TEM (figure 2).

BET surface areas (including the total and external surface area) and pore volumes of the HBeta zeolites with different particle sizes are given in table 1. All three kinds of zeolites are similar in the BET surface areas (ca. 590 m^2/g). However, they are quite different in the external surface areas and the pore volumes that may be assigned to the inter-particulate spaces; the external surface areas increase considerably from 97 m^2/g, 114 m^2/g, to 130 m^2/g and the pore volumes from 0.29 cm^3/g, 0.47 cm^3/g, to 0.68 cm^3/g for zeolites from β_L (2.3–4.0 μm), β_M (210–300 nm), to β_S (60–100 nm), respectively.

NH_3-TPD profiles of HBeta zeolites with different particle sizes are shown in figure 3. Normally, NH_3-TPD profiles of HBeta zeolites suggest two desorption peaks; they are located in the regions of low-temperature (LT, below 400 °C) and high-temperature (HT, above 400 °C), respectively [20,21]. These two distinct bands at around 240 and 400 °C are attributed to desorption of NH_3 from weak Lewis acid sites and decomposition of NH_4^+ ions formed over strong acid sites, respectively [22]. The NH_3-TPD profiles suggest that three HBeta zeolites of different particle sizes exhibit little difference in the acid properties (strength and density). As also listed in table 1, the densities of acid sites are about 5.60 mmol/g for all three HBeta zeolites.

3.2. Catalytic activity and stability

The acylation of toluene with acetic anhydride was carried out at 130 °C with a molar ratio of toluene to acetic anhydride of 10. As shown in table 2, acylated toluene is the major product. The products distribution shows that the ratio of *para*- to *ortho*-MAP is 98:2 and no metaisomer is detected. Nano-sized β_S gives the highest yield of acylated products; there is an obvious decrease in the yield of acylated products with increasing the particle size of zeolites. Because three HBeta zeolites of different particle sizes own similar acid properties and density of active sites, as suggested by the NH_3-TPD profiles, the high activity of nano-sized zeolites might come from more accessible active sites and/or reduced diffusion limitation, which allows a much easier access of reactants to the active sites and leaving of heavy products from the catalyst surface [23].

The acylation of more reactive reactant anisole with acetic anhydride was carried out in a fixed-bed reactor at 120 °C with a molar ratio of anisole to acetic anhydride of 5. For all tests in this work, the selectivity towards *p*-MOAP is about 98% and keeps at this value with the time on stream. However, the conversion of acetic

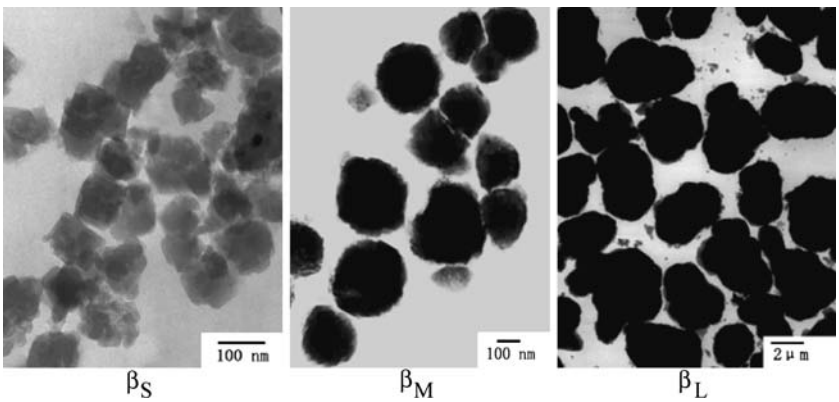

Figure 2. TEM of the as-synthesized Beta zeolites (β_S, nano-sized; β_M, medium sized; β_L, large sized).

Table 1
Properties of HBeta zeolites of different particle sizes[a]

Zeolites	β_S	β_M	β_L
SiO_2/Al_2O_3 mole ratio	33	33	33
$TEAOH/SiO_2$ mole ratio	0.115	0.085	0.180
Na_2O/SiO_2 mole ratio	0.059	0.059	0.094
Relative crystallinity	118	100	63
Particle size range (nm)	60–100	210–300	2300–4000
BET surface area (m^2/g)	595	596	581
External surface area (m^2/g)	130	114	97
Pore volume (cm^3/g)	0.68	0.47	0.29
Density of total acid sites (mmol/g)	5.590	5.601	5.605
Surface area, spent catalyst[b] (m^2/g)	227	215	200
Pore volume, spent catalyst[b] (cm^3/g)	0.65	0.33	0.12

[a]Nano-sized β_S and medium sized β_M are synthesized by surface wet method, while large sized β_L is synthesized by the nucleation gel method.
[b]Spent catalysts are the catalysts after enduring the acylation of anisole with acetic anhydride for 30 h on stream at 120 °C.

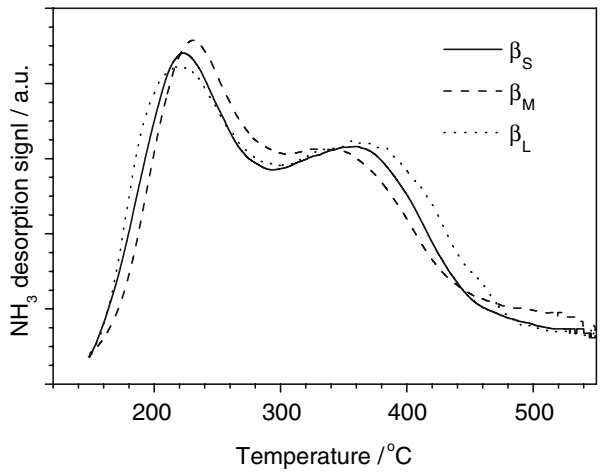

Figure 3. NH_3-TPD profiles of HBeta zeolites of different particle sizes (β_S, nano-sized; β_M, medium sized; β_L, large sized).

Table 2
Acylation of toluene with acetic anhydride over the HBeta zeolites of different sizes[a]

Zeolites	MAP Yield (%)[b]	Product distribution (%)	
		para-MAP	*ortho*-MAP
β_S	71.1	98.0	2.0
β_M	64.3	96.0	4.0
β_L	57.3	98.0	2.0

[a]Reaction conditions: 0.1 g catalyst, 60 mmol toluene and 6 mmol acetic anhydride were charged in a 20 ml autoclave; reaction lasted for 3 h at 130 °C and 0.13 MPa.
[b]Methylacetophenone (MAP) yield is based on the reactant acetic anhydride.

anhydride depends on both the particle size of zeolites and the time on stream. As shown in figure 4, the highest activity and stability are obtained on the nano-sized catalyst β_S; the conversion of acetic anhydride at beginning is 93.0%, decreases slowly with the time on stream and then keeps at about 57.7% after 33 h on stream. Although β_M and β_L exhibit a similar initial conversion of acetic anhydride (95% and 92%, respectively, at 1 h on stream) as β_S, their activities, especially the activity of β_L, decrease drastically with the time on stream. After 33 h on stream, the conversions of acetic anhydride over β_M and β_L decrease to 37.1% and 7.0%, respectively; this indicates a serious catalyst deactivation.

Three kinds of HBeta zeolites with different crystal sizes give the similar *p*-MOAP selectivity and initial acetic anhydride conversion, indicting that the particle size and external surface area have little influence on the nature of the active sites in these zeolites. On the other hand, the selectivity towards *p*-MOAP remains the same for the three Beta zeolites with time on steam, indicating that the external surface of the catalyst has little contribution to the acylation. This observation has been also reported in the reaction of phenol hydroxylation over TS-1 zeolites [13]. Thus, the high activity of nano-sized zeolites may be ascribed mainly to the improved efficiency of the active sites as a result of better accessibility and less diffusion limitation.

3.3. Catalyst deactivation

With Beta zeolites as catalyst for acylation, the molecular sizes of reactants and products are comparable to the pore openings of zeolites; their diffusion in zeolites is therefore strongly inhibited by the small pore size. The strong adsorption of products such as *p*-MOAP on the active sites, which endured further reaction to form heavier products, is responsible for catalyst deactivation [5,11,24]. The accumulation of heavier products inside the pores may partly block the pore access and result in the irreversible deactivation of catalyst. Derouane *et al.* [5] found that for the acylation of anisole over HBeta zeolites, the adsorption of *p*-MOAP on the active sites is preferential to those of the reactants acetic anhydride and anisole, and then attributed the decrease in the activity to the decrease in the

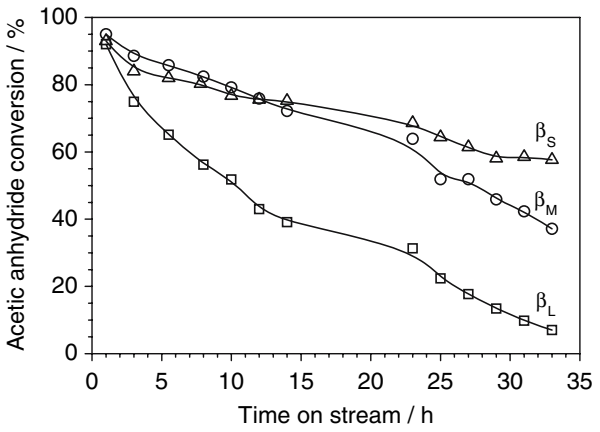

Figure 4. Catalytic tests for the acylation of anisole with acetic anhydride over Beta zeolites of different particle sizes (β_S, nano-sized; β_M, medium sized; β_L, large sized) in a fixed bed reactor at 120 °C and 3.7 MPa (the initial molar ratio of anisole/acetic anhydride is 5 and the weight hourly space velocity is 10 h^{-1}).

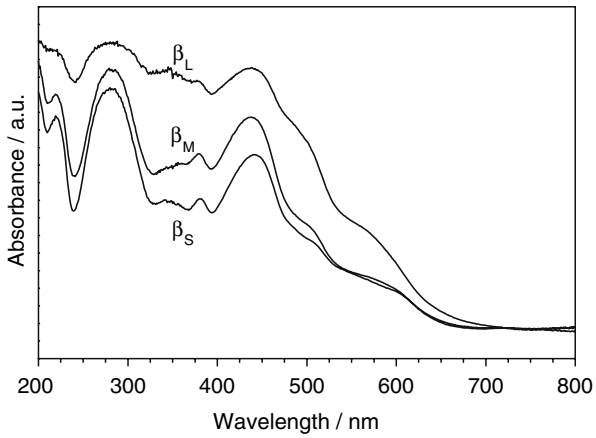

Figure 5. UV–VIS spectra of the spent catalysts of different particle sizes (β_S, nano-sized; β_M, medium sized; β_L, large sized) after the acylation of anisole with acetic anhydride for 33 h on stream.

accessibility of active sites to the reactants. Rohan *et al.* [11] reported that the byproducts with large molecules, formed from the polyacetylation of anisole, block the micropores of zeolites and prohibit the reactants from accessing to the active sites.

The lifetime of zeolite catalysts may be prolonged by reducing their particle size or using the zeolites of large pore size. Winé *et al.* [25] reported that the rapid evacuation of heavy ketone products from catalyst may help to improve the acylation stability of Beta zeolites (with the particle size of around 30 nm) supported on a β-SiC foam monolith in the benzoylation of anisole. Yamamura *et al.* [15] suggested that the lifetime of ZSM-5 zeolite in the oligomerization of ethylene depends on the large external surface area of zeolites with small particle size. Berrichi *et al.* [24] reported that Ga doped SBA-15 mesoporous silica exhibits relatively higher stability than HBeta zeolites, which is attributed to the presence of mesoporous network in SBA-15 that favors the diffusion of reactants and products.

The surface area and pore volume of spent catalysts after the acylation of anisole with acetic anhydride for 33 h on stream at 120 °C are also listed in table 1. The surface area of the catalysts decreases considerably after enduring the reaction, indicating a heavy blockage in the micropore of the zeolites. On the other hand, the pore volume of catalyst β_S after enduring the reaction remains at the same level as that of fresh catalyst, while the pore volumes of β_M and β_L decreased largely after enduring the reaction. This suggests a less deposition of heavy products on β_S than that on β_M or β_L.

The UV–VIS spectra of the spent catalysts after the acylation of anisole with acetic anhydride for 33 h on stream at 120 °C are depicted in figure 5. There are two distinct absorption bands centered at 270 and 435 nm, respectively. The absorption band at 270 nm is originated from the product *p*-MOAP adsorbed on the catalyst. The band at 435 nm probably comes from the presence of condensed aromatic compounds, typical carbonaceous deposits [26]. It is evident that the absorbances at 270 and 435 nm increase with the particle size of Beta zeolites. Therefore, high stability of β_S with small particle size for the acylation is associated with the fewer amounts of *p*-MOAP adsorbed and coke deposited on the catalyst.

DTG and CO_2 signal for TG-MS measurement of the spent catalysts after the acylation of anisole with acetic anhydride for 33 h on stream are illustrated in figure 6. The weight loss around 200 °C is attributed to the desorption of adsorbed water and *p*-MOAP, while that at about 500 °C can be ascribed to the combustion of condensed aromatic compounds deposited on the catalyst. The amounts of coke deposition on β_S, β_M and β_L are 9.7, 10.3 and 10.6 wt%, respectively. In addition, the temperature of coke combustion shifts to higher value for zeolites from β_S, β_M to β_L, indicating that the coke deposited on β_L is much heavier than those on small-sized zeolites [25].

The nano-sized Beta zeolites as catalysts exhibit much higher activity and stability in the acylation than the zeolites of larger particle sizes. This can be ascribed to the improved efficiency of the active sites as a result of better accessibility and less diffusion limitation. With zeolites of small particle sizes as catalysts, the heavy products such as *p*-MOAP and ketones produced from the acylation reaction can escape from micropores in zeolites much more easily; this prevents the heavy products from occupying the active sites and further forming cokes that may block the access of reactants to the active sites. These may alleviate the deactivation of catalyst considerably.

4. Conclusions

Nano-sized Beta zeolites with a crystal size of 80–100 nm were synthesized via surface wet method.

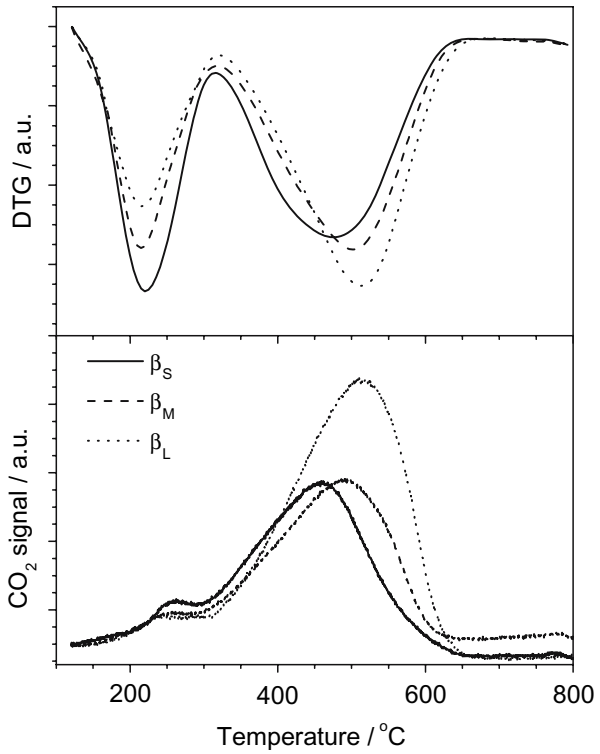

Figure 6. DTG (upper) and CO_2 signal (lower) for the TG-MS measurement of the spent HBeta catalysts after the acylation of anisole with acetic anhydride for 33 h on stream (solid line, nano-sized β_S; dash line, medium sized β_M; dotted line, large sized β_L).

Their catalytic performances on the Friedel–Crafts acylation of anisole or toluene with acetic anhydride were investigated comparatively with those of medium (210–300 nm) large (2.3–4.0 μm) sized Beta zeolites.

The nano-sized HBeta zeolites exhibit much higher activity and stability in the Friedel–Crafts acylation than the conventional large particle sized zeolites. The small crystal size of nano-sized zeolites may bring on more accessible active sites and then enhance the catalytic activity. The exposed pore openings in nano-sized zeolites allow a fast desorption of heavy products from the catalyst and can then reduce the occupancy of active sites by the adsorption of products; this can then alleviate the catalyst deactivation and improve the catalyst stability.

Acknowledgments

The authors are grateful for the financial support of the Sate Key Fundamental Research Project (2006CB202504) and the Natural Science Foundation of China (20473110, 20603044) and Shanxi Province.

References

[1] G.A. Olah, *Friedel–Crafts and Related Reactions*, (Wiley-Interscience, New York, 1963).
[2] P. Metivier, in: *Fine Chemicals through Heterogeneous Catalysis*, eds., R.A Sheldon and H. van Bekkum (Wiley-VCH, Weinheim, Germany, 2001).
[3] U. Freese, F. Heinrich and F. Roessner, Catal. Today 49 (1999) 237.
[4] A.E.W. Beers, J.A. van Bokhoven, K.M. de Lathouder, F. Kapteijn and J.A. Moulijn, J. Catal. 218 (2003) 239.
[5] E.G. Derouane, C.J. Dillon, D. Bethell and S.B. Derouane-Abd Hamid, J. Catal. 187 (1999) 209.
[6] P.B. Venuto, Micropor. Mater. 2 (1994) 297.
[7] J. Kaur and I.V. Kozhevnikov, Chem. Commun. 21 (2002) 2508.
[8] B.M. Devassy, S.B. Halligudi, S.G. Hegde, A.B. Halger and F. Lefebvre, Chem. Commun. 10 (2002) 1074.
[9] B. Bachiller-Baeza and J.A. Anderson, J. Catal. 228 (2004) 225.
[10] M. Kodomari, Y. Suzuki and K. Yoshida, Chem. Commun. 16 (1997) 1567.
[11] D. Rohan, C. Canaff, E. Fromentin and M. Guisnet, J. Catal. 177 (1998) 296.
[12] M.A. Camblor, A. Corma, A. Martinez, V. Martinez-Soria and S. Valencia, J. Catal. 179 (1998) 537.
[13] A.J.H.P. van der Pol, A.J. Verduyn and J.H.C. van Hooff, Appl. Catal. A 92 (1992) 113.
[14] K. Beschmann and L. Riekert, J. Catal. 141 (1993) 548.
[15] M. Yamamura, K. Chaki, T. Wakatsuki, H. Okada and K. Fujimoto, Zeolites 14 (1994) 643.
[16] G.H. Liu, M.Y. He, X.T. Shu, L.H. Zuo and Y. Gao, Chinese Patent, CN 96100045.7 (1996).
[17] Q. Zhou, B.I. Li, S.L. Qiu and W.Q. Pang, Chem. J. Chinese Univers. 20 (1999) 693.
[18] M.A. Camblor, A. Mifsud and J. Pérez-Pariente, Zeolites 11 (1991) 792.
[19] L.H. Ding, Y. Zheng, Z.S. Zhang, Z. Ring and J.W. Chen, Micropor. Mesopor. Mater. 94 (2006) 1.
[20] M. Sawa, M. Niwa and Y. Murakami, Zeolites 10 (1990) 532.
[21] H. Sato, Catal. Rev.-Sci. Eng. 39 (1997) 395.
[22] F. Lonyi and J. Valyon, Thermochim. Acta 373 (2001) 53.
[23] K. Rajagopalan, A.W. Peters and G.C. Edwards, J. Catal. 23 (1986) 69.
[24] Z.E. Berrichi, L. Cherif, O. Orsen, J. Fraissard, J.P. Tessonnier, E. Vanhaecke, B. Louis, M.J. Ledoux and C. Pham-Huu, Appl. Catal. A 298 (2006) 194.
[25] G. Winé, J.P. Tessonnier, S. Rigolet, C. Marichal, M.J. Ledoux and C. Pham-Huu, J. Mol. Catal. A 248 (2006) 113.
[26] M. Rozwadowski, M. Lezanska, J. Wloch, K. Erdmann, R. Golembiewski and J. Kornatowski, Chem. Mater. 13 (2001) 1609.